

# Preparation of a hierarchically porous AlPO<sub>4</sub> monolith via an epoxide-mediated sol–gel process accompanied by phase separation

Wenyan Li<sup>1,2</sup>, Yang Zhu<sup>2</sup>, Xingzhong Guo<sup>1</sup>, Kazuki Nakanishi<sup>2</sup>, Kazuyoshi Kanamori<sup>2</sup> and Hui Yang<sup>1</sup>

<sup>1</sup> Department of Materials Science and Engineering, Zhejiang University, Hangzhou, 310027, People's Republic of China

<sup>2</sup> Department of Chemistry, Graduate School of Science, Kyoto University, Kitashirakawa, Sakyo-ku, Kyoto 606–8502, Japan

E-mail: [gxzh\\_zju@163.com](mailto:gxzh_zju@163.com) and [kazuki@kuchem.kyoto-u.ac.jp](mailto:kazuki@kuchem.kyoto-u.ac.jp)

Received 22 April 2013

Accepted for publication 4 July 2013

Published 1 August 2013

Online at [stacks.iop.org/STAM/14/045007](http://stacks.iop.org/STAM/14/045007)

## Abstract

Monolithic aluminum phosphate (AlPO<sub>4</sub>) with a macro–mesoporous structure has been successfully prepared via the sol–gel process accompanied by phase separation in the presence of poly(ethylene oxide) (PEO). Gelation of the system has been mediated by propylene oxide (PO), while PEO induces a phase separation. The dried gel is amorphous, whereas the crystalline tridymite phase precipitates upon heating above 1000 °C. Heat treatment does not spoil the macroporous morphology of the AlPO<sub>4</sub> monoliths. Nitrogen adsorption–desorption measurements revealed that the skeletons of the dried gels possess a mesostructure with a median pore size of about 30 nm and a surface area as high as 120 m<sup>2</sup> g<sup>−1</sup>. Hydrothermal treatment before heat treatment can increase the surface area to 282 m<sup>2</sup> g<sup>−1</sup>.


Keywords: aluminum phosphate, monolith, porous, sol–gel, phase separation

## 1. Introduction

Aluminum phosphate, AlPO<sub>4</sub>, is a compound with solid bi-functional acid–bases, and has been known as an important candidate for catalyst supports or molecular sieves because of its zeolite-like structure and special properties [1–16]. For example, AlPO<sub>4</sub> has been used to catalyze the oxidation reaction of alkanes, cycloalkanes and phenols by loading transition metals in its network.

As an advanced catalyst support, AlPO<sub>4</sub> has attracted considerable attention. Arita [17] has reported the effective

use of a tridymite-form of AlPO<sub>4</sub> as the catalyst in converting glycerol into acrolein. Itoh *et al* [18] reported that compared with other ortho- and pyro-phosphates such as CePO<sub>4</sub>, CeP<sub>2</sub>O<sub>7</sub>, SnP<sub>2</sub>O<sub>7</sub>, TiP<sub>2</sub>O<sub>7</sub> and Zn<sub>3</sub>(PO<sub>4</sub>)<sub>2</sub> as a support for a Pt catalyst, Pt/AlPO<sub>4</sub> has the best activity of deNO<sub>x</sub> and high-activity-desorbed ammonia at a higher temperature. He and co-workers [19] reported that using AlPO<sub>4</sub> as the carrier can decrease the elution of Ag<sup>+</sup> for its excellent adsorption and ion exchange. Machida *et al* [20] showed that AlPO<sub>4</sub> is an efficient and robust support material to produce optimum metal–support interactions that can reduce Rh loading significantly. However, little attention has been paid to macroporous AlPO<sub>4</sub> materials, and the AlPO<sub>4</sub> monoliths with hierarchically porous structures have not been reported in the open literature.

 Content from this work may be used under the terms of the Creative Commons Attribution-NonCommercial-ShareAlike 3.0 licence. Any further distribution of this work must maintain attribution to the author(s) and the title of the work, journal citation and DOI.

**Table 1.** Starting compositions and resultant morphology of the dried samples.

Sample	AlCl <sub>3</sub> ·6H <sub>2</sub> O(g)	H <sub>3</sub> PO <sub>4</sub> (ml)	H <sub>2</sub> O(ml)	MeOH(ml)	PO(ml)	PEO(mg)	Morphology
APO-1	0.500	0.1418	0.4863	0.30	0.40	8.90	nano-pores
APO-2	0.500	0.1418	0.4863	0.30	0.40	10.20	co-continuous
APO-3	0.500	0.1418	0.4863	0.30	0.40	10.55	co-continuous
APO-4	0.500	0.1418	0.4863	0.30	0.40	10.75	co-continuous
APO-5	0.500	0.1418	0.4863	0.30	0.40	11.00	co-continuous
APO-6	0.500	0.1418	0.4863	0.30	0.40	11.20	isolated pores
APO-7	0.500	0.1418	0.4863	0.30	0.38	11.00	particles
APO-8	0.500	0.1418	0.4863	0.30	0.42	11.00	isolated pores
APO-9	0.500	0.1418	0.4863	0.38	0.40	24.70	co-continuous

Porous materials have been paid much attention in both scientific research and practical applications [21–25]. For a catalyst support, a hierarchically porous structure and monolithic shape are more meaningful and desirable. In hierarchically porous monoliths, large pores such as macropores allow facile fluid transport, while the presence of additional mesopores gives rise to a large surface area and more reaction sites. A sol–gel process accompanied by phase separation is known to be one of the more-promising techniques for fabricating hierarchically porous monoliths. In this approach, the phase separation and sol–gel transition concur by a polymerization reaction to produce a wet gel with a co-continuous structure, in which each of the gel-rich and solvent-rich phases is interconnected on the length scale of a micrometer. Subsequent solvent exchange of the macropores with a basic aqueous solution and heat treatment yields mesopores with diameters of 5–10 nm via a process known as Ostwald ripening, without essentially disturbing the macroporous structures. This reliable and reproducible method has also been applied to prepare porous monoliths such as SiO<sub>2</sub> [26], TiO<sub>2</sub> [27–30], ZrO<sub>2</sub> [31], Al<sub>2</sub>O<sub>3</sub> [32], yttrium aluminum garnet [33], Fe<sub>3</sub>O<sub>4</sub> [34], and even LiFePO<sub>4</sub> [35] and CaHPO<sub>4</sub> [36]. Hirayama and Yamada [37] reported that macroporous AlPO<sub>4</sub> monoliths can be prepared from aluminum nitrate nonahydrate, dihydrogen ammonium phosphate and poly(ethylene oxide). However, there have been no studies on mesopore modification by hydrothermal ageing.

In this paper, we demonstrate a novel and facile method for the preparation of hierarchically porous AlPO<sub>4</sub> monoliths by combining the phase separation with the sol–gel route. A system with inexpensive chloride salts as an additional precursor is adopted to synthesize the AlPO<sub>4</sub> monoliths in the presence of propylene oxide (PO) and poly(ethylene oxide). The resulting AlPO<sub>4</sub> monoliths possess precisely controllable macropores and mesostructured skeletons, precise control of macropores by PO-mediated gelation and hydrothermal ageing to tailor mesopore distribution. A lot of benefits are expected to arise from the co-continuous structure integrated in monoliths. Moreover, mesoporous aluminum organophosphonates are also reported [38–41], and we deduced that aluminum organophosphonates can also be prepared by phase separation with the sol–gel route.

## 2. Experimental details

### 2.1. Materials

The starting compositions of the samples are listed in table 1. AlCl<sub>3</sub>·6H<sub>2</sub>O (Sigma-Aldrich, 99%) and H<sub>3</sub>PO<sub>4</sub> (Sigma-Aldrich, ≥ 85 wt% solution in water) were utilized as aluminum and phosphorous sources. Mixtures of distilled water and methanol (MeOH: Kishida Chemical, 99.8%) were used as the solvents. Propylene oxide (PO: Sigma-Aldrich, ≥ 99%) was added as a proton scavenger for the purpose of modifying the rate of pH increase. Poly(ethylene oxide) (PEO: Sigma-Aldrich) with molecular weight ( $M_v$ ) of  $1 \times 10^4$  was used as a phase-separation inducer. All chemicals were used as received.

### 2.2. Synthesis of monoliths

The detailed preparation of the gel was as follows. Appropriate amounts of H<sub>2</sub>O, MeOH, H<sub>3</sub>PO<sub>4</sub> and PEO were mixed with AlCl<sub>3</sub>·6H<sub>2</sub>O while stirring under ice-cooled conditions. After stirring for 15 min, PO was added slowly (about 1 ml min<sup>-1</sup>) with vigorous stirring. After mixing for 30 s, the obtained homogeneous solution was degassed by ultra-sonication for 10 s in order to remove bubbles and then was sealed and allowed to gel at 40 °C. The resultant wet gel was aged at 40 °C for 24 h, solvent exchanged by 2-propanol two times and evaporation-dried at 40 °C for 5 days. Some of the dried gels were heat treated at various temperatures between 800 and 1100 °C for 10 h in air at a heating rate of 275 °C min<sup>-1</sup>.

Some of the APO-9 wet gels were immersed in 0.1, 0.3, 0.5, 0.7 and 1.0 mol l<sup>-1</sup> NH<sub>4</sub>OH solutions at 40 °C three times. Then the gel and solvent were together transferred into a stainless-steel autoclave vessel with a Teflon inner liner and additionally aged at 100 and 120 °C for 3 h under an autogeneous pressure in order to tailor the micro and mesoporous structures. The hydrothermally aged gel thus obtained was solvent-exchanged with distilled water and 2-propanol, and was evaporation-dried at 40 °C for 5 days.

### 2.3. Characterization

The microstructure of the fractured surfaces of the samples was observed using a scanning electron microscope (SEM);

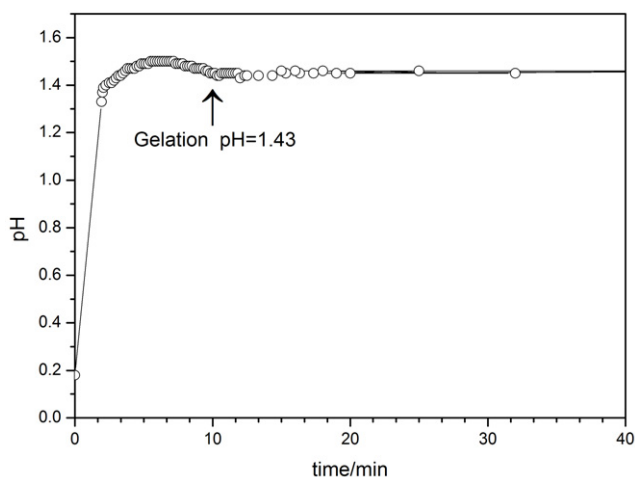


**Figure 1.** pH value as a function of time after the addition of propylene oxide.

JSM-6060, JEOL Ltd, Akishima, Japan). The crystal structure was confirmed by powder x-ray diffraction (XRD) (RINT Ultima III, Rigaku Corp., Japan) using a  $\text{CuK}\alpha$  radiation ( $\lambda = 0.154 \text{ nm}$ ) source as an incident beam. The change of the pH value during the sol–gel reaction was measured at  $40^\circ\text{C}$  using an F-21 (HORIBA, Ltd, Kyoto, Japan) pH meter. Nitrogen adsorption–desorption apparatus (Belsorp mini II, Bel Japan Inc., Toyonaka, Japan) was used to characterize the meso- and micropores of the samples. Before each nitrogen adsorption–desorption measurement, the sample was degassed at  $200^\circ\text{C}$  under a vacuum for more than 8 h. The pore size distribution was calculated from the adsorption branch of the isotherm by the Barrett–Joyner–Halenda (BJH) method, and the surface area was obtained by the Brunauer–Emmett–Teller (BET) method.

### 3. Results and discussion

#### 3.1. Macroporous morphology of monoliths

In this system, the hydrolysis of aluminum chloride ( $\text{AlCl}_3 \cdot 6\text{H}_2\text{O}$ ) in the mixture of  $\text{H}_2\text{O}$  and  $\text{MeOH}$  will produce abundant  $\text{H}^+$  and  $\text{Cl}^-$  to make the solution highly acidic. At the same time, the hydrolysis products, such as hydrated  $\text{Al}^{3+}$ , will react with  $\text{PO}_4^{3-}$  to form  $\text{AlPO}_4$ . Homogeneous and transparent solutions were prepared. When propylene oxide (PO) was added to the solution and time elapsed, the phase separation and the gelation proceeded spontaneously in a closed and static condition at a constant temperature ( $40^\circ\text{C}$ ). The gelation and phase separation could be controlled by the concentrations of PO and PEO. As reported, the sol–gel reaction is triggered by an increase in the pH induced by the ring-opening reaction of propylene oxide, which acts as an irreversible acid scavenger [42–44].

Experimentally, as shown in figure 1, we found that after the addition of PO, the pH value dramatically increases from 0.18 to 1.50 in the initial stage because of the ring-opening reaction of the PO, and then decreases slightly. The gelation takes place at  $\text{pH} \sim 1.43$ , and the time required is about 10 min.

In contrast, the addition of PEO did not have an important effect on the gelation time, but induced the phase separation to form a macroporous structure after drying. When the phase-separation is induced by the sol–gel reaction in the presence of PEO, the well-defined two-phase structure in the form of a co-continuous structure is developed, which is the result of spinodal decomposition. Subsequent sol–gel transition fixes the co-continuous structure, which is converted into well-defined macroporous monoliths after the removal of the solvent phase. The phase separation tendency is related to the miscibility of a polymeric system, which can be estimated by the Flory–Huggins formulation [45–47]. The Gibbs free energy change of mixing,  $\Delta G$ , can be described as follows:

$$\Delta G \propto RT \left( \frac{\varphi_1}{P_1} \ln \varphi_1 + \frac{\varphi_2}{P_2} \ln \varphi_2 + \chi \varphi_1 \varphi_2 \right), \quad (1)$$

where  $\varphi_i$  and  $P_i$  are the volume fraction and the degree of polymerization of component  $i$  ( $i = 1$  or  $2$ ), respectively,  $\chi$  is the interaction parameter,  $R$  is the gas constant and  $T$  is the temperature. The former two terms in parentheses represent the entropic contribution, and the last term the enthalpic contribution. In the  $\text{SiO}_2$  system in the presence of poly(acrylic acid), the phase separation is driven by the entropy loss due to the polymerization of  $\text{SiO}_2$  oligomers, whereas the enthalpy-driven phase separation is observed for the PEO-incorporated  $\text{SiO}_2$  systems, where there exists a repulsive interaction between the solvent mixture and the PEO adsorbed on  $\text{SiO}_2$  oligomers [26]. In the present system, a similar repulsive interaction is expected to work for the present PEO-incorporated  $\text{AlPO}_4$  oligomers via hydrogen bonding.

Figure 2 shows SEM images of dried gels prepared with various amounts of PEO. As the amount of PEO increases, the structures of the dried gels change from those with nanopores, through co-continuous skeletons and pores, to a continuous gel matrix with isolated pores. This reflects that the tendency for phase separation increases. When phase separation occurs much later than gelation, transparent gels with nanometer-sized pores can be obtained as monoliths. Nearly concurrent sol–gel transition and phase separation produce co-continuous structures (figures 2(b)–(e)), in which each of the gel phase and the fluid phase is three-dimensionally interconnected on the length scale of micrometers. After evaporation drying, the fluid phase is composed mainly of solvent mixture transformed into continuous macropores, and the gel phase becomes skeletons.

The increase in the amount of PO effectively shortens the gelation time because the PO accelerates the pH increase. The effect of the amount of PO on the gel morphologies was also investigated, as shown in figure 3. The structure changes from fine aggregated particles through co-continuous structures to the coarse isolated macropores with an increase of PO concentration. Taking into account the fact that gelation is accelerated by increasing the concentration of PO, the onset of phase separation should be made still earlier than gelation with PO concentration. In addition, the volume fraction of the solvent phase (non-gelling phase) drastically decreases with PO concentration. The effect of PO is more complex than the



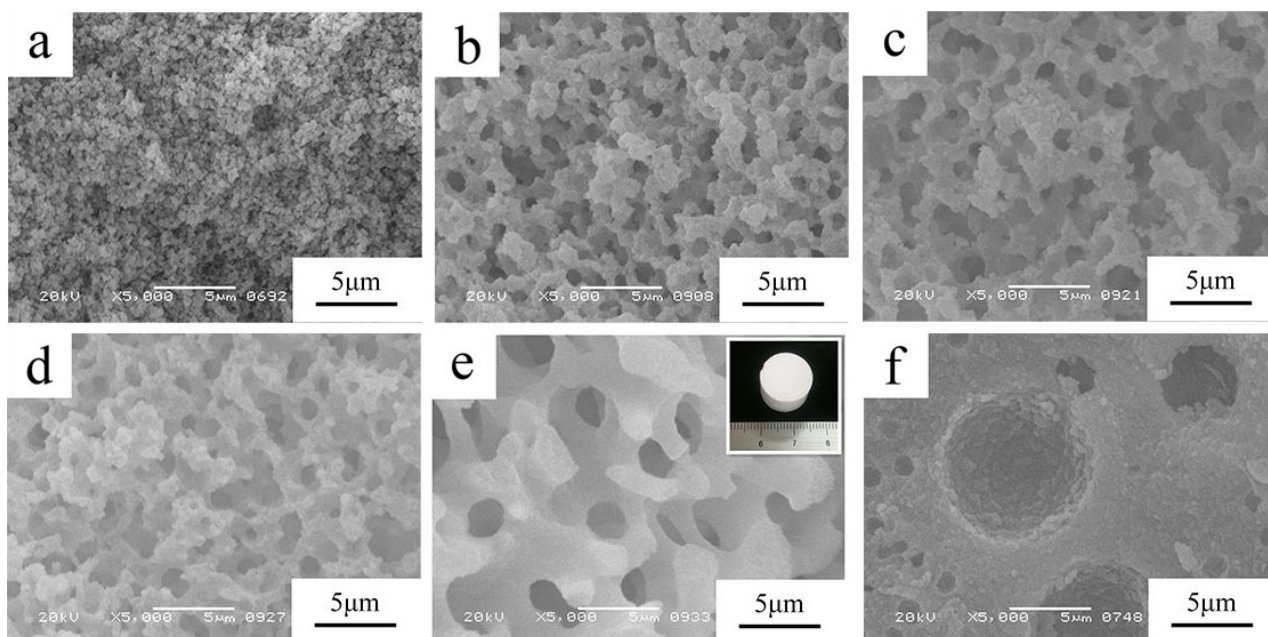


**Figure 2.** Scanning electron micrographs of the dried  $\text{AlPO}_4$  gels prepared with varied polyethylene oxide contents. (a)  $w_{\text{PEO}} = 8.90$  mg; (b)  $w_{\text{PEO}} = 10.20$  mg; (c)  $w_{\text{PEO}} = 10.55$  mg; (d)  $w_{\text{PEO}} = 10.75$  mg; (e)  $w_{\text{PEO}} = 11.00$  mg; (f)  $w_{\text{PEO}} = 11.20$  mg.

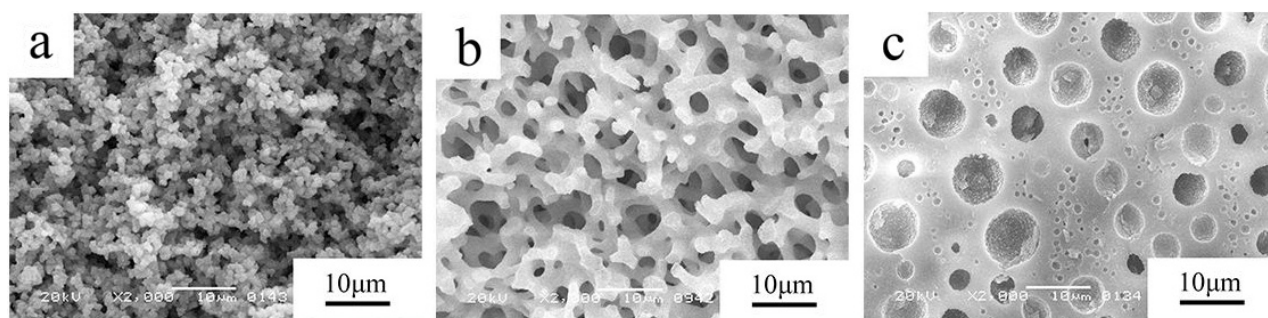


**Figure 3.** Macroporous structure of the  $\text{AlPO}_4$  dried gels with varied PO amounts. (a) 0.38 ml; (b) 0.40 ml; (c) 0.42 ml.

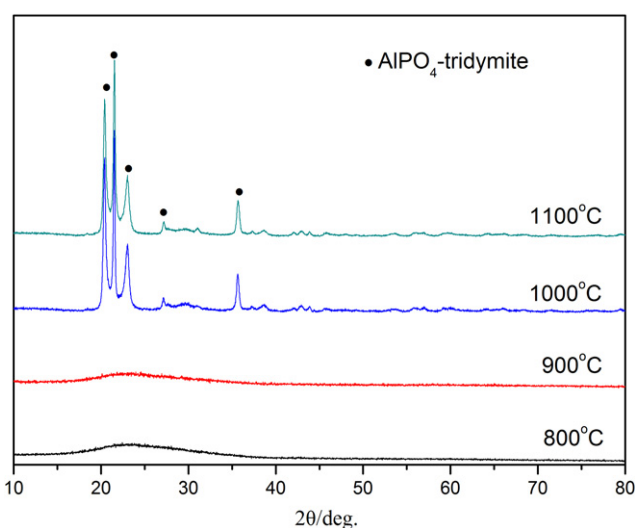
case of a pure alumina system possibly because  $\text{AlPO}_4$  has much lower solubility in an aqueous system [32].

### 3.2. Heat treatment of monoliths

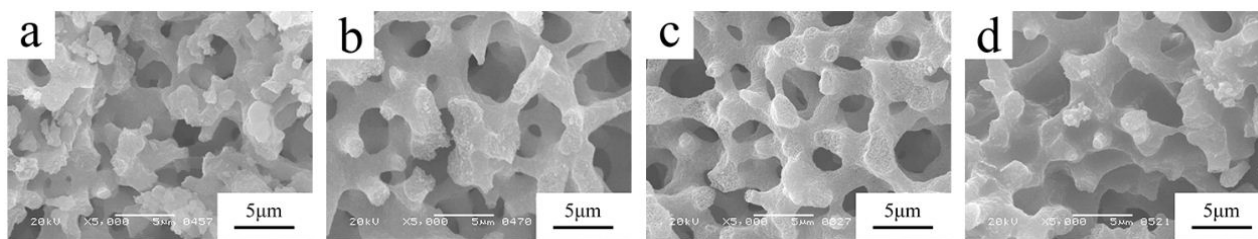
The heat treatment of the APO-5 dried gel with  $w_{\text{PEO}} = 11.00$  mg was carried out at various temperatures, at 100 °C intervals between 800 and 1100 °C, holding the temperature for 8 h with a heating rate of 275–276  $\text{K min}^{-1}$ , and the effects of heat treatment on the crystallinity and micro and mesoporous structure were examined.

Figure 4 displays the XRD patterns of the gels heat treated at various temperatures. There are no discernible peaks found for the gels heat treated at 800 and 900 °C, indicating an amorphous structure, or one with very fine crystallites; whereas the diffraction peaks ascribed to tridymite-type  $\text{AlPO}_4$  appear after heat treatment at 1000 and 1100 °C.

Figure 5 shows macroporous morphologies of the gels calcined at different temperatures. It is found that



**Figure 4.** X-ray diffraction patterns of the  $\text{AlPO}_4$  samples calcined at different temperatures.



**Figure 5.** Morphologies of the cross section of the skeletons calcined at different temperatures. (a) 800 °C; (b) 900 °C; (c) 1000 °C; (d) 1100 °C.

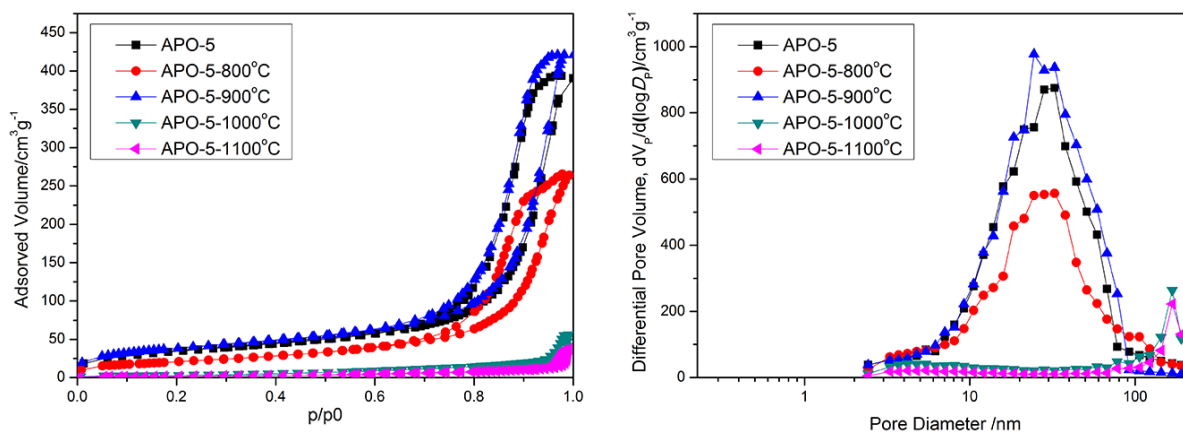


**Figure 6.** Pore characterizations of the  $\text{AlPO}_4$  gels at different heat-treatment temperatures.

**Table 2.** Pore characteristics of the  $\text{AlPO}_4$  monoliths calcined at different temperatures.

Sample	Heat-treatment temperature (°C)	$S_{\text{BET}}$ ( $\text{m}^2 \text{g}^{-1}$ )	$V_p$ ( $\text{cm}^3 \text{g}^{-1}$ )
APO-5	200	120	0.5882
	800	74	0.4104
	900	139	0.6419
	1000	15	0.0895
	1100	8	0.0570

the well-defined co-continuous macroporous morphology is basically maintained after heat treatment in the range of 800–1100 °C, indicating that the formation of a crystalline phase does not spoil the macroporous morphology of  $\text{AlPO}_4$  monoliths.

Figure 6 shows  $\text{N}_2$  adsorption–desorption isotherms and the corresponding BJH pore-size distribution of the APO-5 sample with  $w_{\text{PEO}} = 11 \text{ mg}$  at different heat treatment temperatures. The uptake at very low relative pressure is derived from the existence of micropores. Compared with the sample without heat treatment, the shape of the adsorption–desorption isotherm after heat treatment at 800 and 900 °C does not change obviously, and the uptake at a relative pressure higher than 0.8 disappears at 1000 and 1100 °C, indicating the elimination of mesopores. The pore characteristics are summarized in table 2. The surface area of APO-5 at 200 °C is as high as  $120 \text{ m}^2 \text{g}^{-1}$ . It is seen that the surface area first decreases at 800 °C,

and immediately increases to a maximum value at 900 °C, and then dramatically decreases with further increase in heat-treatment temperature. The decrease in surface area after calcination at 800 °C is due to large shrinkage and the increase in surface area at 900 °C is attributed to the formation of  $\text{AlPO}_4$  nanocrystals; the gaps between nanocrystals contribute to the surface area and pore volume. However, the surface area and pore volume decreases with further increase in heat-treatment temperature because of the growth of nanocrystals and the sintering of skeletons.

### 3.3. Hydrothermal treatment

We investigated the effects of post-gelation treatment on co-continuous macroporous APO-9 wet gel with  $w_{\text{PEO}} = 24.70 \text{ mg}$  using a hydrothermal process in order to obtain the mesostructure on the skeletons, without spoiling the macrostructure. Figure 7 shows the macroporous structure of the  $\text{AlPO}_4$  gels without or with hydrothermal treatment; it does not spoil the macroporous morphology of the  $\text{AlPO}_4$  monoliths even at the condition of  $1.0 \text{ mol l}^{-1} \text{NH}_4\text{OH}$  solution at 120 °C.

In contrast, the hydrothermal treatment has an important influence on the mesopores of the  $\text{AlPO}_4$  monoliths. Figure 8 shows the pore characteristics of an  $\text{AlPO}_4$  wet gel with  $w_{\text{PEO}} = 24.70 \text{ mg}$  under different hydrothermal treatment conditions; the pore characteristics are summarized in table 3. The dried and hydrothermally treated gels exhibit isotherms of type-IV with an H1 hysteresis loop, signifying the existence of

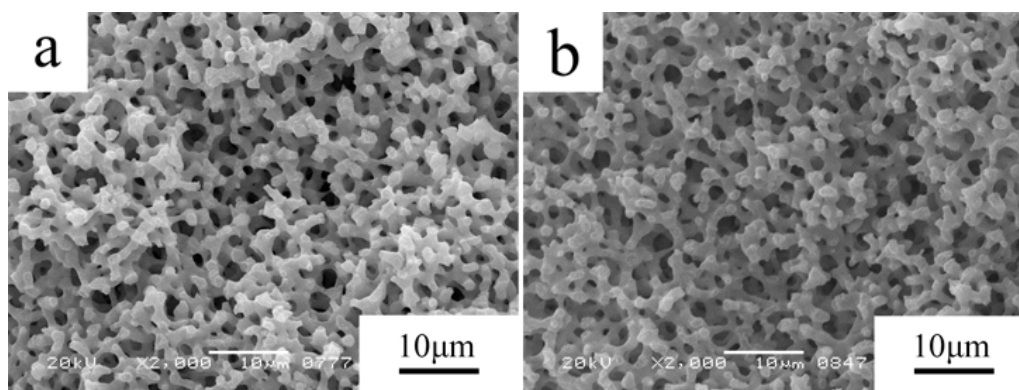


**Figure 7.** Macroporous structure of the AlPO<sub>4</sub> gels without or with hydrothermal treatment. (a) Without hydrothermal; (b) 120 °C, 1 mol l<sup>-1</sup> NH<sub>4</sub>OH.

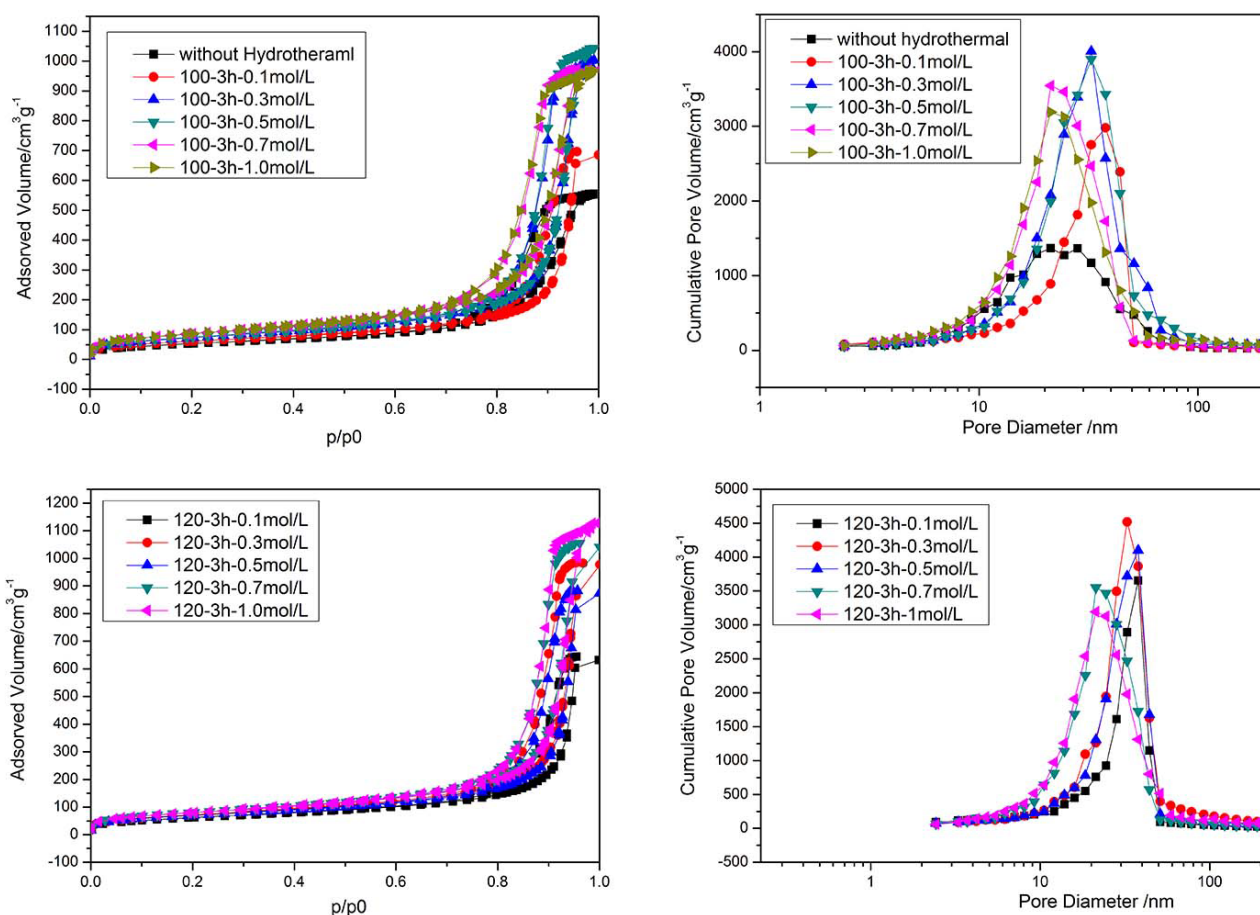


**Figure 8.** Pore characterizations of the AlPO<sub>4</sub> gels for different treatment conditions.

mesopores. Hydrothermal treatment promotes the production of mesopores and obviously increases the pore volume and surface area. It is also confirmed by the corresponding pore-size distribution curves. Compared with the dried gel (figure 6), the gels after hydrothermal treatment show a relatively narrow pore-size distribution. The surface areas and mesopore volume increase with the increase of NH<sub>4</sub>OH concentration. The precise control of the volume and the size distribution of the mesopores will be carried out by careful

processing under appropriate conditions. The highest surface area of the gel can reach 282 m<sup>2</sup> g<sup>-1</sup>.

The continuous gel framework contains inherent vacant spaces in the nanometer length scale that are filled with solvents in the wet state. On evaporation drying, however, most of these spaces are collapsed by capillary forces. Weakly basic aqueous solutions in the temperature range up to 120 °C can modify micropores into mesopores larger than 15 nm in diameter. According to the classical Ostwald ripening theory,



**Table 3.** Pore characteristics of the AlPO<sub>4</sub> monoliths treated at different conditions.

Sample	Hydrothermal temperature (°C)	NH <sub>3</sub> (mol l <sup>-1</sup> )	Time (h)	S <sub>BET</sub> (m <sup>2</sup> g <sup>-1</sup> )	V <sub>p</sub> (cm <sup>3</sup> g <sup>-1</sup> )
APO-9	–	–	–	176	0.90
	100	0.1	3	200	1.04
	100	0.3	3	244	1.55
	100	0.5	3	247	1.61
	100	0.7	3	280	1.49
	100	1.0	3	282	1.50
	120	0.1	3	203	0.95
	120	0.3	3	237	1.46
	120	0.5	3	229	1.32
	120	0.7	3	265	1.57
	120	1.0	3	262	1.73

the dissolution is most enhanced on the sharp points with the smallest positive curvature, whereas the reprecipitation is most pronounced at the cavities with the smallest negative curvature. As a result, with an elapse of hydrothermal treatment ageing, the finer roughness is removed and the whole surface is reorganized into one with only coarser points and cavities. In the case where three-dimensional networks of AlPO<sub>4</sub> gels are present, smaller pores are eliminated and the whole pore system is reorganized into one with larger mesopores, possibly distributed in the size range greater than 50 nm.

#### 4. Conclusions

Monolithic AlPO<sub>4</sub> gels with co-continuous macropores and mesopores have been prepared via the sol–gel process mediated by propylene oxide (PO) in the presence of poly(ethylene oxide) (PEO), and the micro- and mesotextures of the gel skeletons have been tailored by utilizing hydrothermal ageing as a post-gelation process.

Adjustment of the concentrations of PEO and PO in the starting solution allows concurrence of polymerization-induced phase separation and gelation, and produces monolithic gels with controllable macroporous morphology. Hydrothermal ageing of the wet gels in weakly basic conditions at 100 and 120 °C enlarges the size of the mesopores without spoiling the macroporous morphology, the degree of which is dependent on the concentration of NH<sub>4</sub>OH and the ageing temperature. The present synthetic process thus enables us to produce crack-free AlPO<sub>4</sub> monoliths having meso–macroporous structures with adjustable pore sizes and uniform pore-size distributions.

#### References

- [1] Danjo Y, Kikuchi I, Ino Y, Ohshima M A, Kurokawa H and Miura H 2012 *React. Kinetics. Mech. Catal.* **105** 381
- [2] Fujii R, Seki M, Shinoda J, Okazaki N and Tada A 2003 *Chem. Lett.* **32** 764
- [3] Rigutto M S and van Bekkum H 1993 *J. Mol. Catal.* **81** 77
- [4] Lertjamratn K, Praserttham P, Arai M and Panpranot J 2010 *Appl. Catal. A: Gen.* **378** 119
- [5] Javid M 2006 *J. Chem. Soc. Pakistan* **28** 323 ([jcspp.org.pk/ArticleUpload/1069-4744-1-RV.pdf](http://jcspp.org.pk/ArticleUpload/1069-4744-1-RV.pdf))
- [6] Kimura T 2005 *Micropor. Mesopor. Mater.* **77** 97
- [7] Kimura T, Sugahara Y and Kuroda K 1999 *Chem. Mater.* **11** 508
- [8] Campelo J M, Jaraba M, Luna D, Luque R, Marinas J M, Romero A A, Navio J A and Macias M 2003 *Chem. Mater.* **15** 3352
- [9] Tian B Z, Liu X Y, Tu B, Yu C Z, Fan J, Wang L M, Xie S H, Stucky G D and Zhao D Y 2003 *Nature. Mater.* **2** 159
- [10] Tian D, Yan W, Cao X, Yu J and Xu R 2008 *Chem. Mater.* **20** 2160
- [11] Chary K V R, Kishan G, Ramesh K, Kumar C P and Vidyasagar G 2003 *Langmuir* **19** 4548
- [12] Tiemann M and Froba M 2001 *Chem. Mater.* **13** 3211
- [13] Cabello J A, Campelo J M, Garcia A, Luna D and Marinas J M 1984 *J. Org. Chem.* **49** 5195
- [14] Wilson S T, Lok B M, Messina C A, Cannan T R and Flanigen E M 1982 *J. Am. Chem. Soc.* **104** 1146
- [15] Mishra T, Parida K M and Rao S B 1998 *Appl. Catal. A: Gen.* **166** 115
- [16] Ashtekar S, Barrie P J, Hargreaves M and Gladden L F 1997 *Angew. Chem. Int. Edn Engl.* **36** 876
- [17] Arita Y 2009 Method of synthesizing acrolein from glycerol Patent P2009–57305A Japan
- [18] Itoh M, Takehara M, Saito M, Machida K and IOP 2011 *3rd Int. Congress on Ceramics* vol 18
- [19] Chang Q, He H, Zhao J, Yang M and Qu J 2008 *Environ. Sci. Technol.* **42** 1699
- [20] Machida M, Murakami K, Hinokuma S, Uemura K, Ikeue K, Matsuda M, Chai M, Nakahara Y and Sato T 2009 *Chem. Mater.* **21** 1796
- [21] Shiba K, Tagaya M, Tilley R D and Hanagata N 2013 *Sci. Technol. Adv. Mater.* **14** 023002
- [22] Yu Y, Addai-Mensah J and Losic D 2012 *Sci. Technol. Adv. Mater.* **13** 015008
- [23] Vivero-Escoto J L, Chiang Y D, C-Wwu K and Yamauchi Y 2012 *Sci. Technol. Adv. Mater.* **13** 013003
- [24] Suzuki N, Sakka Y and Yamauchi Y 2009 *Sci. Technol. Adv. Mater.* **10** 025002
- [25] Vinu A, Mori T and Ariga K 2006 *Sci. Technol. Adv. Mater.* **7** 753
- [26] Nakanishi K 1997 *J. Porous. Mater.* **4** 67
- [27] Hasegawa G, Kanamori K, Nakanishi K and Hanada T 2010 *J. Am. Ceram. Soc.* **93** 3110
- [28] Konishi J, Fujita K, Nakanishi K and Hirao K 2006 *Chem. Mater.* **18** 6069
- [29] Konishi J, Fujita K, Nakanishi K and Hirao K 2004 *Mater. Res. Soc. Symp. Proc.* **788** 391
- [30] Fujita K, Konishi J, Nakanishi K and Hirao K 2006 *Sci. Technol. Adv. Mater.* **7** 511
- [31] Konishi J, Fujita K, Oiwa S, Nakanishi K and Hirao K 2008 *Chem. Mater.* **20** 2165
- [32] Tokudome Y, Fujita K, Nakanishi K, Miura K and Hirao K 2007 *Chem. Mater.* **19** 3393
- [33] Tokudome Y, Fujita K, Nakanishi K, Kanamori K, Miura K, Hirao K and Hanada T 2007 *J. Ceram. Soc. Japan* **115** 925
- [34] Kido Y, Nakanishi K, Miyasaka A and Kanamori K 2012 *Chem. Mater.* **24** 2071
- [35] Hasegawa G, Ishihara Y, Kanamori K, Miyazaki K, Yamada Y, Nakanishi K and Abe T 2011 *Chem. Mater.* **23** 5208
- [36] Tokudome Y, Miyasaka A, Nakanishi K and Hanada T 2011 *J. Sol–Gel Sci. Technol.* **57** 269
- [37] Hirayama T and Yamada I 2011 *9th Annual Meeting of Japanese Sol–Gel Society*, Kansai University (Osaka, Japan)
- [38] Kimura T and Yamauchi Y 2013 *Chem Asian J.* **8** 160

- [39] Kimura T and Yamauchi Y 2012 *Langmuir* **28** 12901
- [40] Kimura T, Suzuki N, Gupta P and Yamauchi Y 2010 *Dalton Trans.* **39** 5139
- [41] Kimura T, Kato K and Yamauchi Y 2009 *Chem. Commun.* **2009** 4938
- [42] Gash A E, Tillotson T M, Satcher J H, Poco J F, Hrubesh L W and Simpson R L 2001 *Chem. Mater.* **13** 999
- [43] Gash A E, Tillotson T M, Satcher J H, Hrubesh L W and Simpson R L 2001 *J. Non-Cryst. Solids* **285** 22
- [44] Itoh H, Tabata T, Kokitsu M, Okazaki N, Imizu Y and Tada A 1993 *J. Ceram. Soc. Japan* **101** 1081
- [45] Huggins M L 1942 *J. Am. Chem. Soc.* **64** 2716
- [46] Huggins M L 1942 *J. Phys. Chem.* **46** 151
- [47] Flory P J 1942 *J. Chem. Phys.* **10** 51